Physicochemical Characterization of Silicalite-1 Nanophase Material

Raman Ravishankar,[†] Christine Kirschhock,[†] Brian J. Schoeman,[‡] Peter Vanoppen,[§] Piet J. Grobet,[†] Sebastian Storck,[||] Wilhelm F. Maier,[||] Johan. A. Martens,*[,†] Frans C. De Schryver,[§] and Pierre A. Jacobs[†]

Departement Interfasechemie, Centrum voor Oppervlaktechemie en Katalyse, K.U. Leuven, Kard. Mercierlaan 92, B-3001 Heverlee, Belgium, Department of Chemical Technology, Luleå University of Technology, Sweden, Laboratorium Moleculaire Dynamica en Spectroscopie, K.U. Leuven, B-3001, Heverlee, Belgium, and Max-Planck-Institut für Kohlenforschung, Mülheim an der Ruhr, Germany

Received: September 29, 1997; In Final Form: December 9, 1997

A silicalite-1 nanophase material with an elementary particle size of 18−100 nm is synthesized from clear solution and isolated and purified using supercentrifugation. The nanopowder is characterized in detail using scanning electron microscopy, high-resolution transmission electron microscopy, attenuated force microscopy, ^{29}Si magic angle spinning NMR, ^{13}C cross polarization magic angle spinning NMR, X-ray diffraction, dinitrogen physisorption, and thermogravimetric analysis and compared with micrometer-sized silicalite-1. The nanosized and micrometer-sized materials have many common properties including the refined structure and the nature and concentrations of tetrapropylammonium species incorporated during the synthesis. Unique properties of the nanophase are a splitting of the characteristic framework vibration at 550 cm^{-1} into a doublet at 555 and 570 cm^{-1}, a high concentration of defect sites, and a strain in the crystallites along the "*a*" crystallographic direction. The nanophase exhibits a two-stage dinitrogen physisorption in the low-pressure region, ascribed to adsorptions in micropores created by the stacking of the nanoparticles in addition to adsorptions in the intracrystalline micropores.

Introduction

The reduced size and dimensions in nanophase materials is at the basis of unique applications in microelectronics, nanocomposites, ultrathin oxide films, and so forth.[1] In the field of synthetic zeolites, there is also a considerable interest in decreasing the particle size from the micrometer to the nanometer scale in order to decrease, for instance, mass- and heat-transfer resistances in catalytic and sorptive processes. The conventional hydrothermal gel method of zeolite synthesis, introduced by Barrer,[2] yields typically micrometer-sized crystals. The syntheses of zeolites were also achieved by using clear solutions instead of gels.[3−7] From clear solutions, nanocrystals of a variety of zeolite materials including silicalite-1,[8−10] Na−ZSM-5,[11] TS-1,[12] sodalite,[13−15] A, Y,[16,17] ZSM-2,[18,19] and $AlPO_4$-5[20] have been synthesized. The particle size of these colloidal zeolites is a few tens of nanometers.

Silicalite-1 is a crystalline microporous polymorph of silicon dioxide with MFI framework topology.[21] The crystal growth process of silicalite-1 has received considerable attention.[22−28] In this paper, we report an in-depth physicochemical characterization of nanophase silicalite-1 material using X-ray diffraction (XRD) and Rietveld structure refinement, high-resolution transmission electron microscopy (HRTEM), attenuated force microscopy (AFM), magic angle spinning nuclear magentic resonance (MAS NMR), dinitrogen physisorption, and FTIR spectroscopy and compare it with the micrometer-sized versions.

* To whom correspondence should be addressed. Telephone: 016/32 16 37. Fax: 016/32 19 98. E-mail: johan.martens@agr.kuleuven.ac.be.
[†] Centrum Oppervlaktechemie en Katalyse.
[‡] Luleå University of Technology.
[§] Laboratorium Moleculaire Dynamica en Spectroscopie.
[||] Max-Planck-Institut für Kohlenforschung.

Experiment and Instumentation

Silicalite-1 Nanophase Synthesis. The synthesis of the silicalite-1 nanophase was performed following a procedure reported earlier.[8−10] An amount of 20.83 g of tetraethyl orthosilicate [TEOS: Acros, 98%] was added dropwise to 18.34 g of tetrapropylammonium hydroxide [TPAOH: Alfa, 40%, containing 8000 ppm of K impurity] in a polypropylene (PP) bottle under vigorous stirring. A quantity of 18.57 g of distilled water was added after 1 h and the mixture stirred vigorously for 24 h at room temperature. The transparent solution was refluxed for 3 days in a preheated oil bath maintained at 373 K. The solids were separated from the mother liquor by repeated centrifugation (12 000 rpm) and washing with distilled water until the final wash water was at pH less than 8. The sample was redispersed in distilled water and freeze-dried. The synthesis yield on silicon basis was >75%. A portion of the freeze-dried sample was calcined in a stream of dinitrogen gas at 823 K for 2 h and, subsequently, in a flow of dioxygen for 10−12 h at the same temperature.

Instrumentation. Particle-size analysis was carried out using a Malvern Zetasizer 5C with a 5-mW He−Ne laser at a wavelength of 633 nm. The instrument was calibrated with a suspension of polystyrene particles of 102 ± 3 nm. Fourier transform infrared spectra were recorded using the KBr wafer technique and a Nicolet 730 FTIR instrument. The spectra were averaged with over 400 scans with a data spacing of 2 cm^{-1} and corrected for the background.

X-ray diffraction profiles of the samples were recorded on a STOE STADI P diffractometer with Cu Kα1 radiation equipped with a position-sensitive detector (D2θ = 5°) with a resolution of 0.02°. Data were collected between the 2θ range 4°−60°. The structure of the sample was refined by Rietveld refinement

S1089-5647(97)03147-7 CCC: $15.00
Published on Web 03/20/1998

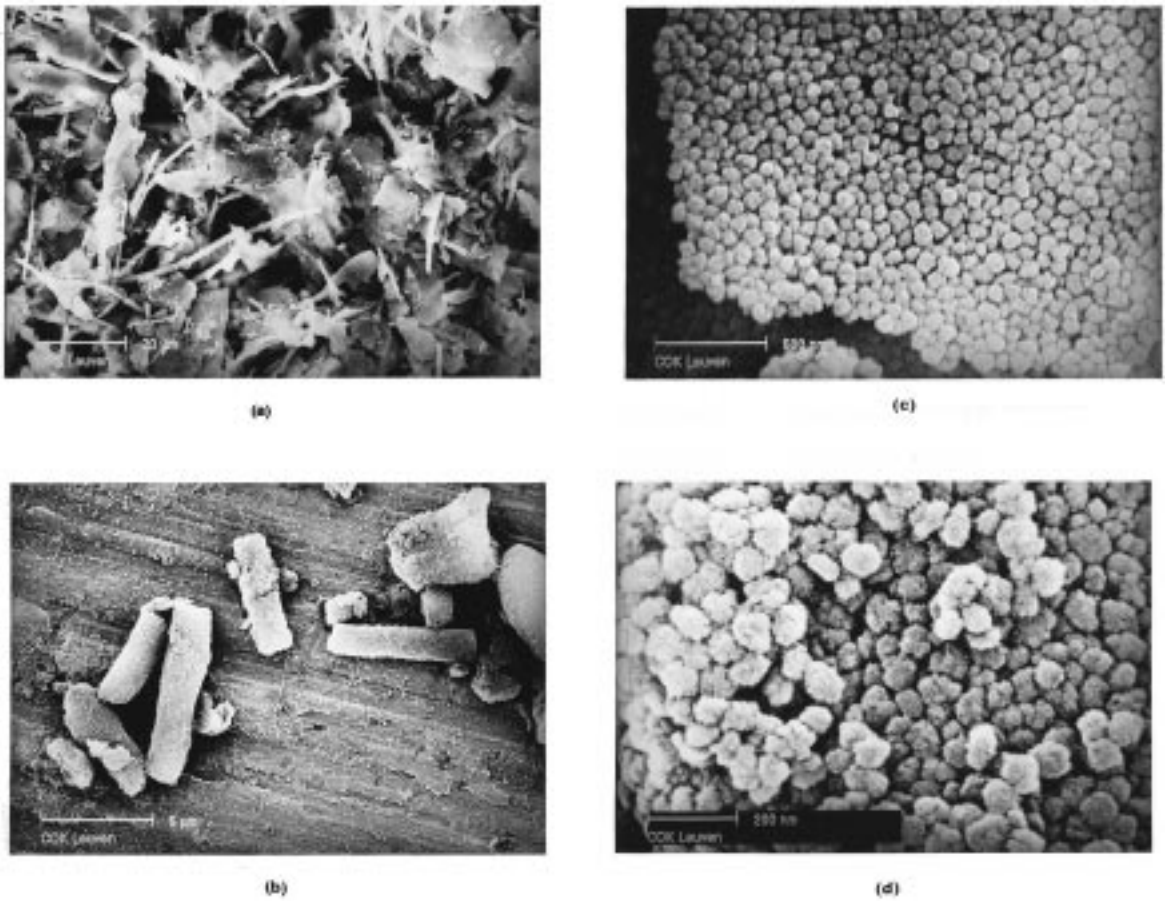

Figure 1. SEM pictures of the calcined colloidal silicalite-1 samples under different magnifications: (a) 1K, (b) 4K, (c) 40K, and (d) 100K times ($1K = 10^3$).

with the GSAS[29] software package using lattice constants and atomic positions reported by van Koningsveld et al.[30]

Scanning electron microscopy (SEM) pictures were taken with a Philips 515 instrument on gold-plated samples. Thermoanalyses were carried out in a Setaram thermogravimetric/differential thermal analysis (TG/DTA) (model 92-12) instrument. The samples were heated from room temperature to 1273 K at a heating rate of 2 K under an atmosphere of 20 vol % dioxygen in helium.

Dinitrogen adsorption isotherms were recorded at 77.23 K using a Micromeretics ASAP 2010 instrument on samples degassed at 400 °C and 0.13 mPa for 10 h.

^{29}Si MAS NMR spectra of the as-synthesized and calcined samples were recorded using a Bruker AMX-300 spectrometer. The ^{29}Si MAS NMR experiments (59.6 MHz) were carried out by means of a 90° single-pulse excitation with a pulse delay of 60 s at a spinning rate of ca. 4 kHz. CP measurements were performed with a contact time of 1 ms and a delay of 3 s. The ^{13}C CP MAS NMR measurements (75.5 MHz) were carried out with a contact time of 3 ms, a delay time of 5 s, and a spinning rate of 4 kHz. In the case of high-power proton-decoupling ^{13}C cross polarization (CP) MAS NMR experiments, a pulse delay of 5 s was found to be adequate to yield quantitatively reliable spectra. TMS was used as the reference for both ^{13}C and ^{29}Si NMR.

AFM experiments were performed with a Discoverer AFM system (TMX 2010, TopoMetrix Inc., Santa Barbara, CA) in noncontact mode using high-frequency (310−380 kHz) cantilevers and amplitude detection. Noncontact cantilevers are equipped with a pyramidal Si_3N_4 tip with a radius of curvature of less than 50 nm. The samples were solvent-casted from chloroform solutions on mica plates.

HRTEM measurements were carried out on a Hitachi HF-2000 instrument combined with energy-dispersive analysis (EDX) at an accelerating voltage of 200 keV. The sample was crushed in an agate mortar in a methanol suspension and transferred to a holey carbon grid (copper, 3-mm diameter).

Results and Discussion

A dilute colloidal silicalite-1 suspension exhibited the Tyndall effect, in agreement with previous observations.[8−10] The hydrodynamic diameter of the suspended particles determined with the Zetasizer was estimated as ca. 90 nm. SEM pictures at different magnifications of the calcined sample are shown in Figure 1. At low magnification (Figure 1a), the sample has the appearance of micrometer-sized thin flakes, which have formed probably during the lyophilization process. The flakes are composed of particles with a uniform size of 50−100 nm (Figure 1), in agreement with previous SEM investigations.[8,9] AFM noncontact imaging revealed that particles of a variety of sizes compose the sample (Figure 2). The smallest particle was found to have a diameter dimension of ∼5 nm, and diameters ranging from 18 to 50 nm were detected typically. Bigger particles (∼90 nm) were present also, and they were always associated with smaller particles (Figure 2). In the HRTEM equipment, at low magnification (75×10^3; 30×10^3 TEM and 2.5 times optical), the same agglomeration of particles with sizes of 50−100 nm was observed (Figure 3a). At magnifications of 750×10^3 (300×10^3 TEM and 2.5 times optical), all particles of 50−100 nm showed lattice planes (Figure 3b). They

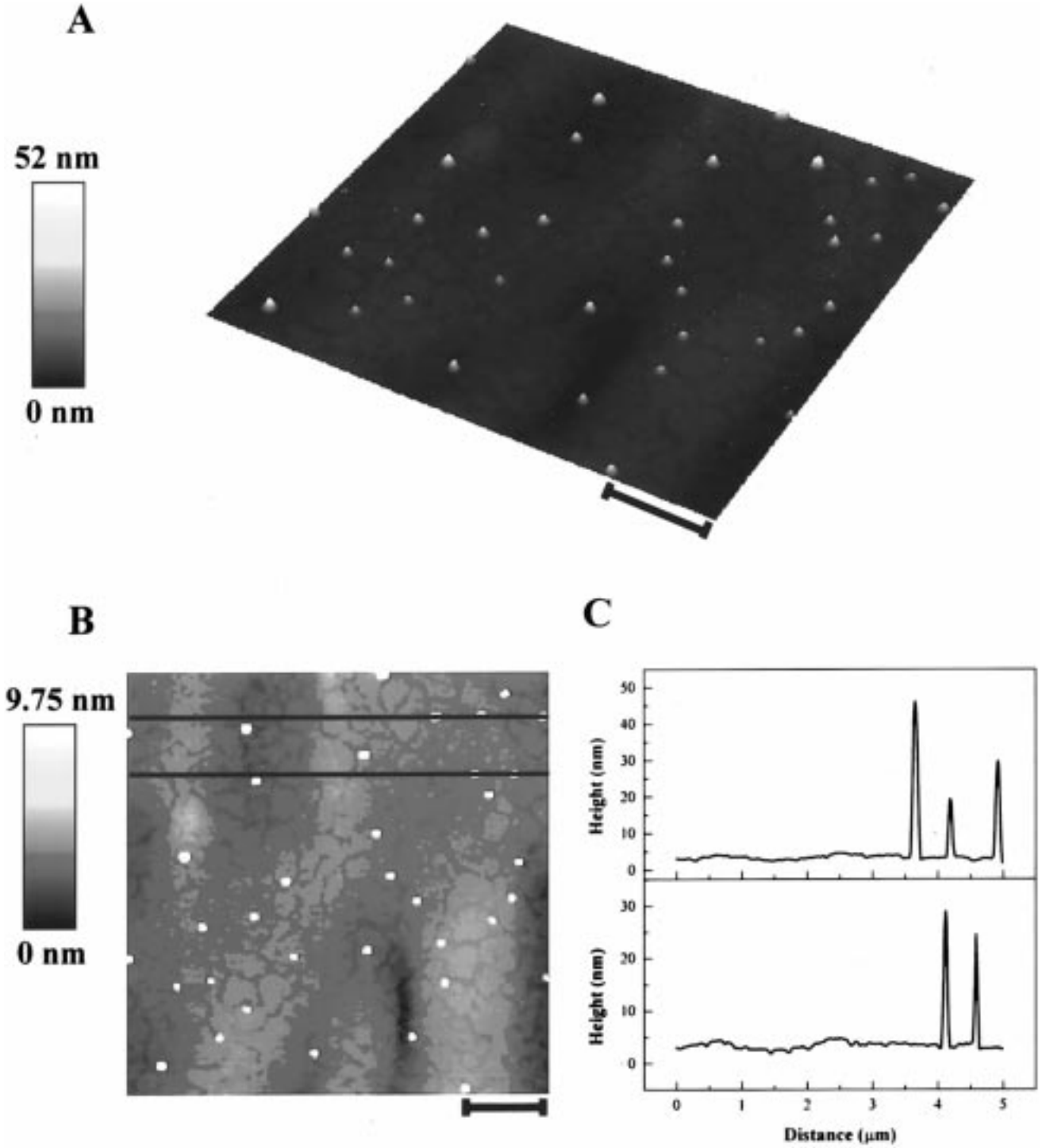

Figure 2. AFM pictures of the calcined colloidal silicalite-1 sample: (A) 3D image of the crystals deposited on the mica plate, where the black scale bar represents 1 μm; (B) 2D display of the same image as in (A) but with different color scale in order to visualize smaller structures in the film; (C) line scans taken at the position of the blue lines in (B) and revealing particle-sizes specimen having crystals of varying heights.

appeared as single crystals without any substructures. The structure of the material broke down and became amorphous within seconds of exposure to the electron beam. The crystalline nature of the particles is well documented in Figure 3c at a total magnification of 60×10^6 (300×10^3 TEM and 20 times video printer). The lattice fringe distance was determined to 0.97 ± 0.03 nm corresponding probably to (200) planes of silicalite-1. In one instance, a particle was found in an orientation parallel to the electron beam, so a view through the pores could be obtained (Figure 3d).

The adsorption isotherm of the calcined sample is shown in Figure 4a. Essentially, it is a type I isotherm according to the classification of Brunauer et al.[31] with a complete filling of the micropore system at very low partial pressures. There is an additional adsorption step at P/P_0 of ca. 0.3 and which is tentatively explained by dinitrogen condensation in pores of 2−3 nm in diameter. This adsorption, which is uncommon for micrometer-sized silicalite-1,[32] must occur in interparticle void spaces present between the elementary crystalline particles. H4-type high-pressure hysteresis typically observed in micrometer-sized MFI phases and ascribed to swelling of microporous fissured regions or between large parallel crystal slabs[32] is not observed. From a *t*-plot analysis of the isotherm according to the method from Lipens and de Boer,[33] Figure 4b, it was

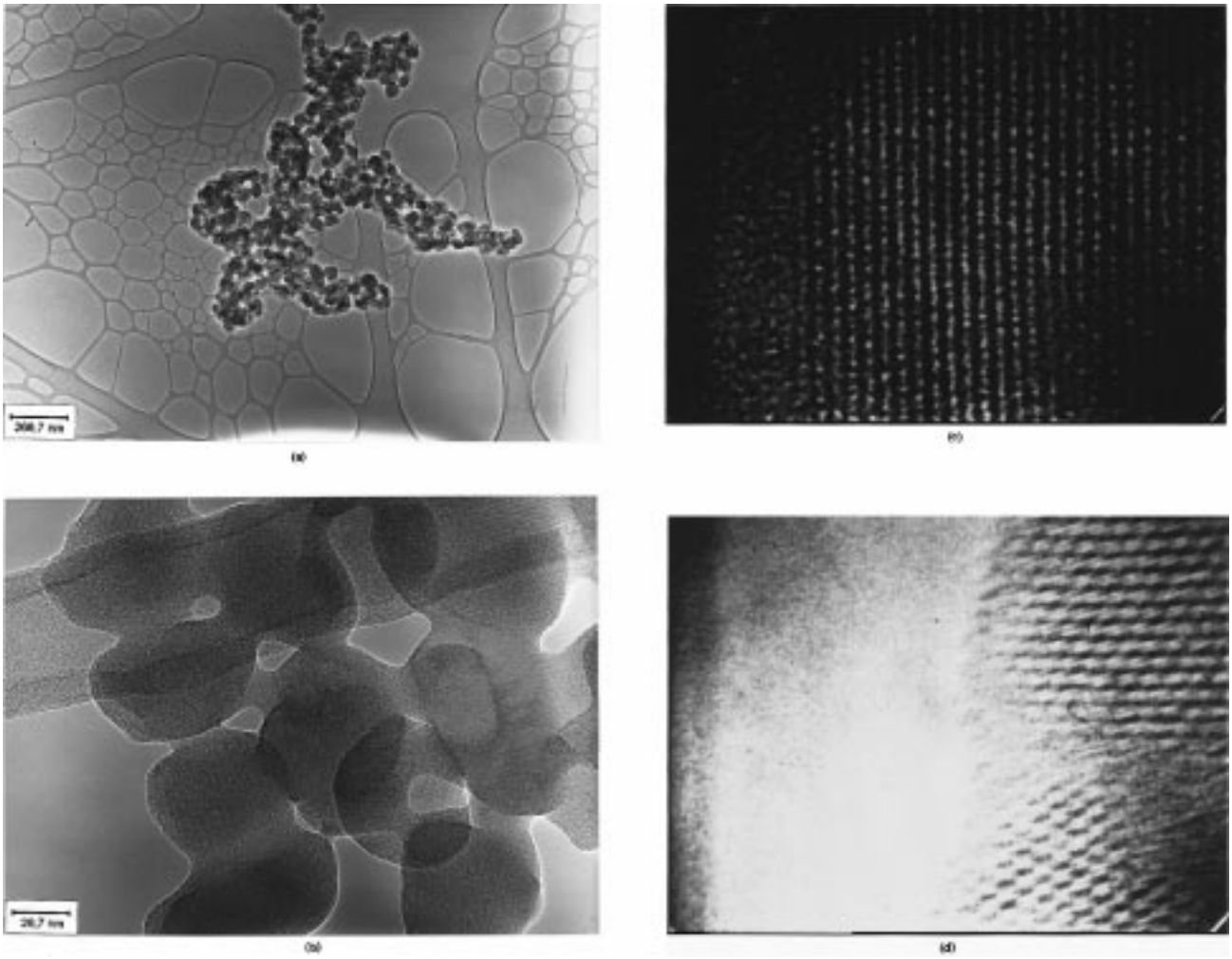

Figure 3. HRTEM images of the calcined sample: (a) cluster of crystals viewed at a magnification of 75K, (b) at a higher magnification of 750K, (c) at 60000K, focusing on a single entity at which lattice planes were revealed, and (d) same magnification showing the pore structure.

derived that the volumes of the smaller and larger micropores correspond to 0.11 and 0.03 cm^3/g, respectively. The specific surface area in the larger micropores is 76 m^2/g, the external specific surface area is 45 m^2/g, and the total surface area in larger micropores and external surface is 121 m^2/g. On the basis of a framework density of 17.9 SiO_2 units per nm^3 and assuming cubic particles for the sake of simplicity, such external surface area corresponds to a particle size of 28 nm, which is in the range of the observations with AFM, SEM, and HRTEM. Corkery and Ninham synthesized 55-nm silicalite-1 particles at low temperature (308 K) and used a very long synthesis time (40 months).[34] The higher external specific surface area of 176 m^2/g found in their sample was ascribed to interstitial void spaces between smaller particles of 5−10 nm composing the 55-nm particles. In our material there is no evidence for such an aggregation of smaller particles.

XRD profiles of the as-synthesized and calcined forms of the sample are shown in Figure 5. In comparison to diffraction patterns of micrometer-sized silicalite-1,[21] the diffraction lines are broadened, in agreement with the results of earlier work.[8−10] Despite the line broadening, the orthorhombic-to-monoclinic phase transformation upon calcination could be observed.

The lattice constants and atomic positions reported by van Koningsveld et al.[30] for uncalcined TPA−silicalite-1 were used as the basic parameters for the refinement of the structure. A unit cell was found to contain four template molecules, each template nitrogen positioned at a channel intersection, and propyl arms stretching in the channels. The position of the template molecule proved to be unstable upon refinement and was held fixed throughout the refinement process. Soft constraints were placed on the T−O distances (1.50 Å < d < 1.68 Å). The weight of these constraints was coupled to ψ^2. The latter parameter decreases with increasing goodness of fit. The refined T−O range was found to be between 1.56 and 1.68 Å, with an average T−O distance per tetrahedron of 1.5999 Å ranging between 1.58 and 1.63 Å. The O−T−O angles varied between 98° and 120°, with an average O−T−O angle per tetrahedron of 109.46° ranging between 109.3° and 109.7°. All atomic parameters of the host lattice except for the O_6 (oxygen-6) were refined. The latter tended to assume a position directly between the T sites 2 and 6 (T_2 and T_6), leading to improbable angles and distances. The crystal symmetry was orthorhombic with a *Pnma* space group. The unit-cell parameters were "a" = 20.0484(25) Å, "b" = 19.9525(24) Å, and "c" = 13.3837(17) Å (estimated standard deviation (esd) of the last digit is in brackets), respectively. These values agree well with the earlier reported values for micrometer-sized silicalite-1.[21,30]

The powder pattern could be refined with one reflection profile function over the refined regions between 7° and 60°. Assuming a strain in the particles along "a" resulted in better R factors, R_{wp} and R_p were reduced by 1% when ψ^2 was changed from 1.5 to 0.8. Final R factors were R_{wp} = 2.2%, R_p = 1.6%, and R_f = 1.7%.[35]

The structure of the calcined sample has not been refined.

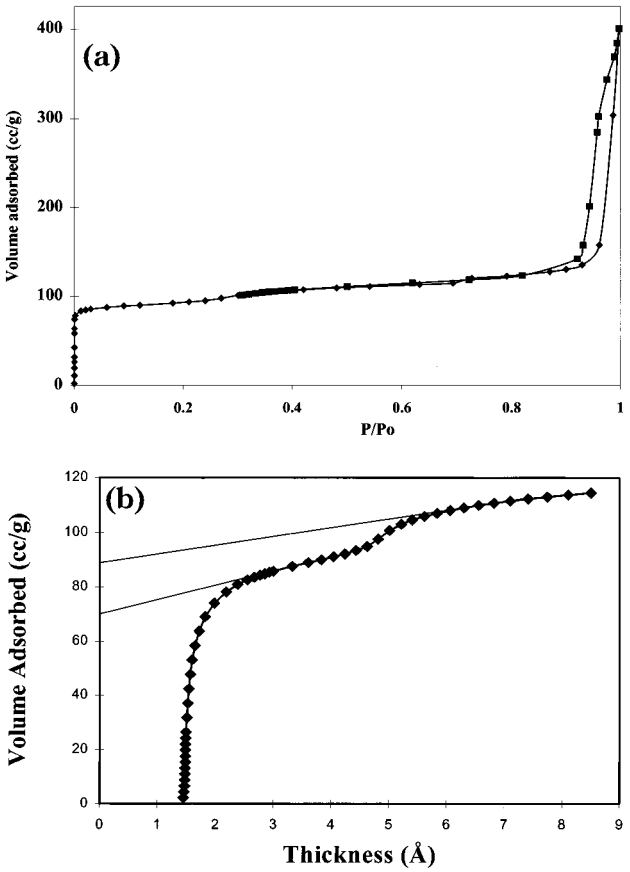

Figure 4. (a) Sorption isotherm of N_2 at 77.23 K over the calcined sample: (◆) adsorption; (■) desorption isotherms. (b) *t* plot according to the method of Lipens and de Boer.[33]

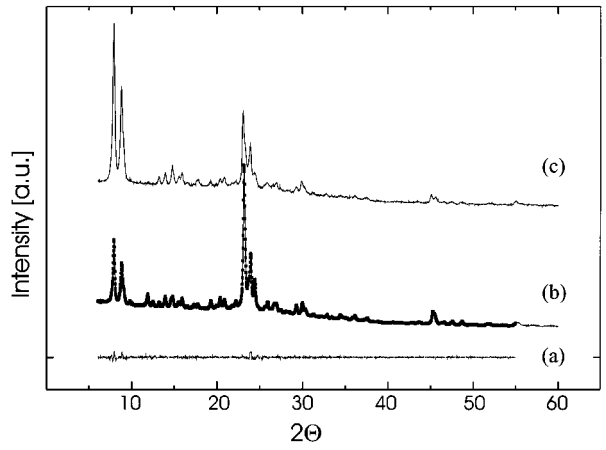

Figure 5. Rietveld refined XRD patterns: (a) Reitveld refinement ($I_{obs} - I_{cal}$) of the as-synthesized form; (b) refined pattern of the as-synthesized form [(−) I_{cal} and (■) I_{obs}]; (c) unrefined pattern of the calcined form [I_{obs}].

The lattice constants were refined using the silicon positions reported earlier.[36] The crystal symmetry and space group of the calcined sample were monoclinic and ($P2_1/n$), respectively, with "*a*" = 20.070(22) Å, "*b*" = 19.887(29) Å, "*c*" = 13.384(16) Å, and β = 90.68(8)° (esd of the last digit in brackets). The peak broadening observed in the calcined sample could be linked to framework deformation upon removal of the template.

^{29}Si NMR spectra of the as-synthesized and calcined samples are presented in Figure 6. In the as-synthesized sample, two broad resonances are observed with chemical shifts of −112 ppm (I) and −103 ppm (II), respectively. Resonance II

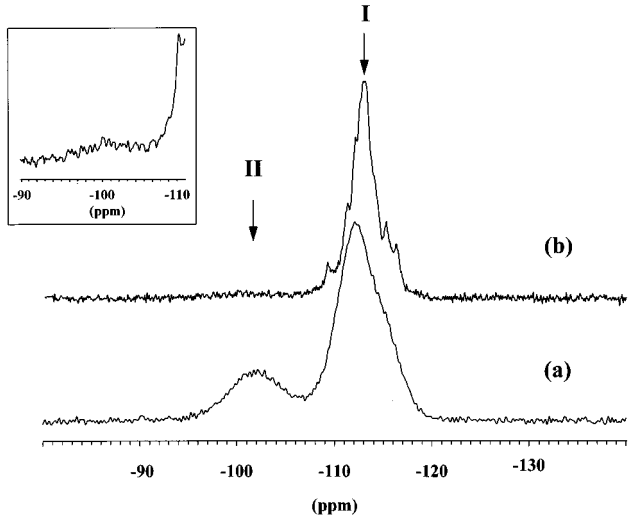

Figure 6. ^{29}Si MAS NMR spectra of colloidal silicalite-1: (a) as-synthesized and (b) calcined forms. Regions I and II are centered at δ = −112 and −103 ppm, respectively. The inset is an enlargement of the region II of spectrum b

represents 19.8% of the total signal. These resonances are attributed to Q^4 silicons (I) and Q^3 silicons (II), respectively. These assignments are based on earlier work[37−40] and were confirmed with the aid of the ^{1}H−^{29}Si cross-polarization technique. Upon calcination, the resonance at δ = −103 ppm reduces to ca. 5% of the intensity, the Q^4 resonance envelope sharpens, and a fine structure owing to the 24 crystallographically inequivalent sites for Si in the framework[41] becomes visible.

The location of the Q^3 silicons can be either at the external surface or at internal defects.[42] For MFI-type zeolites, the percentage of silicon atoms terminating the framework (T_s) can be estimated from the mean crystallite size (*D*) expressed in nanometers.[43]

$$T_s(\%) = 181(^1/_D)$$

For a T_s value of 19.8% (Figure 6a), the particle size is estimated to be 9 nm, which is below the particle-size range measured with SEM, HRTEM, AFM, and dinitrogen physisorption. Assuming an average particle size of 28 nm (based on the *t*-plot analysis, vide supra), the T_s value is 6.5%. The remaining 13.3% of the Q^3 sites must be located at internal framework defects, which is larger than typical concentrations found in micrometer-sized samples, for example, 7% in the work of Woolery et al.[44]

The FTIR spectra of as-synthesized and calcined silicalite-1 nanophase samples are shown in Figure 7. The spectra of the nanophase exhibit some differences compared with those of micrometer-sized silicalite-1. First, in the as-synthesized nanosilicalite-1, an intense band at 960 cm^{-1} is present, which is attributed to silanol groups associated with the Q^3 silicon species,[45,46] detected with ^{29}Si MAS NMR. This IR band disappears from the spectrum after calcination, in agreement with the ^{29}Si MAS NMR data (Figure 6b). Second, the framework vibration at 550 cm^{-1}, characteristic of MFI-type zeolites,[45−48] appears as a doublet (555 and 570 cm^{-1}) in as-synthesized and calcined nanophases.

In the TG/DTA analysis of the as-synthesized nanophase in an oxidative atmosphere, three distinct weight losses are observed: endothermic water desorption up to 425 K, endothermic desorption of TPAOH from 425 to 500 K, and

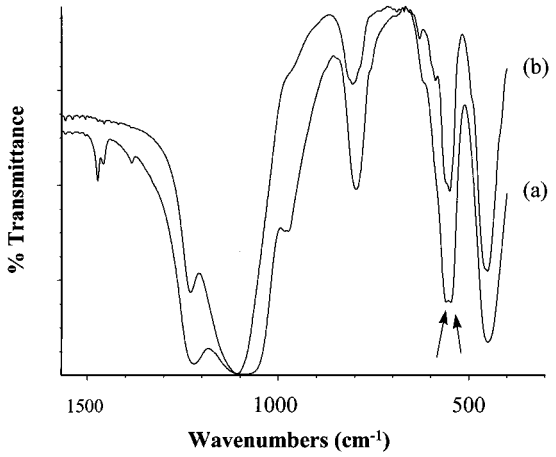

Figure 7. Framework IR spectra of colloidal silicalite-1: (a) as-synthesized and (b) calcined samples. The arrowheads indicate the splitting of the lattice-sensitive band into a doublet (555 and 570 cm^{-1}).

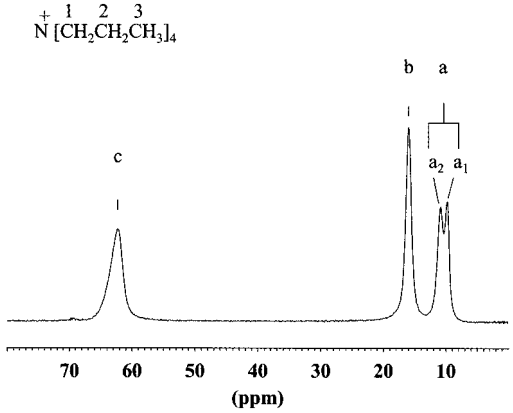

Figure 8. ^{13}C CP MAS NMR spectrum of the as-synthesized form: a_1, $\delta = 9.88$ ppm; a_2, $\delta = 10.95$ ppm; b, $\delta = 16.08$ ppm; c, $\delta = 62.40$ ppm. TMS was used as the standard. Lines a, b, and c are assigned to C^3, C^2, and C^1 of TPA, respectively.

exothermic decomposition of occluded TPAOH molecules at higher temperatures up to 675 K and higher-temperature weight losses to TPA^+ cations balancing negative framework charges at framework interruptions ($Si-O^-$ groups).[42,49]

The TPAOH desorbing at low temperatures represents 1.5 wt % and should be located on the external surfaces of the crystallites. The TPA species occluded in the micropores and giving rise to exothermic weight losses represent 10.7 wt %, or exactly four TPA per unit cell, similar to the values reported in the literature[50] and in agreement with the Rietveld refinement. On the basis of TG/DTA, the nano-silicalite-1 phase contains 2.6 TPAOH and 1.4 TPA^+-SiO^- species per unit cell (96 SiO_2).

The ^{13}C MAS NMR spectrum of the as-synthesized sample (Figure 8) is typical of TPA containing MFI materials.[37] The splitting of the low-field signal has been attributed to the two different locations of the methyl groups (C^3) in the straight and sinusoidal channels of the MFI structure.[38]

Conclusions

According to SEM, HRTEM, AFM, and XRD, silicalite-1 nanophase material consists of elementary crystallites of 18−100 nm. The XRD line broadening is due to the small crystal size. Several properties are not different from larger crystals. The refined structure and the splitting of the ^{13}C CP MAS NMR signal of the C_3 group of the TPA are very similar to that of conventional silicalite-1. The as-synthesized form of the sample contains TPAOH on its external surfaces and TPA occluded in the micropore system. There are 2.6 TPAOH and 1.4 TPA^+-SiO^- species occluded per unit cell. In addition to these TPA^+-SiO^- defects, there are about 13.3 additional Q^3 silicons per unit cell, representing defect sites. Typical of the nanophase is the splitting of the characteristic framework vibration into two bands at 555 and 570 cm^{-1}, the presence of a strain in the "*a*" crystallographic direction, and the presence of an additional step in the dinitrogen physisorption isotherm, ascribed to the presence of larger micropores that are probably located between individual crystallites.

Acknowledgment. This work has been sponsored by the Belgian government in the frame of IUAP-PAI, by the Flemish Fund for Scientific Research (F.W.O. Vlaanderen), and by the Swedish Research Council for Engineering Sciences (TFR). J.A.M. and P.J.G. acknowledge the Flemish Fund for Scientific Research for a research position. R.R. acknowledges K.U. Leuven for a postdoctoral fellowship.

Supporting Information Available: Table of fractional coordinates, isotropic-temperature factors, and occupation numbers of the as-synthesized sample (2 pages). Ordering information is given on any current masthead page.

References and Notes

(1) Goldstein, A. N. *Handbook of Nanophase Materials*; Marcel Decker: New York, 1977.
(2) Barrer, R. M. *Hydrothermal chemistry of zeolites*; Academic Press: New York, 1982.
(3) Ueda, S.; Kageyama, N.; Koizumi, M.; Kobayashi, S.; Fujiwara, Y.; Kyogoku, Y. *J. Phys. Chem.* **1984**, *88*, 2128.
(4) Ueda, S.; Kageyama, N.; Koizumi, M. *Proc. Int. Zeolite Conf., 6th* **1984**, 905.
(5) Szostak, R.; Aiello, R.; Testa, F.; Nastro, A. *Proceedings of the VII European Symposium on Materials and Fluid Sciences in Microgravity*, Brussels, 1992; p 891.
(6) Szostak, R.; Duncan, B.; Aiello, R.; Testa, F.; Nastro, A.; Vinje, K.; Lillirud, K. Molecular Sieves. In *Synthesis of Microporous Materials*; Occelli, Robson, Eds.; Van Nostrand: New York, 1992; Vol. 1, p 240.
(7) Szostak, R. *Molecular Sieves: Principles of synthesis and identification*; Van Nostrand Reinhold Catalysis Series: New York, 1989.
(8) Persson, A. E.; Schoeman, B. J.; Sterte, J.; Otterstedt, J.-E. *Zeolites* **1994**, *14*, 557.
(9) Schoeman, B. J.; Sterte, J.; Otterstedt, J.-E. *Zeolites* **1994**, *14*, 568.
(10) Schoeman, B. J.; Sterte, J.; Otterstedt, J.-E. *J. Porous Mater.* **1995**, *1*, 185.
(11) Persson, A. E.; Schoeman, B. J.; Sterte, J.; Otterstedt, J.-E. *Zeolites* **1995**, *15*, 611.
(12) Zhang, G.; Sterte, J.; Schoeman, B. J. *J. Chem. Soc., Chem. Commun.* **1995**, 3259.
(13) Schoeman, B. J.; Sterte, J.; Otterstedt, J.-E. *J. Chem. Soc., Chem. Commun.* **1993**, 994.
(14) Schoeman, B. J.; Sterte, J.; Otterstedt, J.-E. *Zeolites* **1994**, *14*, 208.
(15) Schoeman, B. J.; Sterte, J.; Otterstedt, J.-E. *Stud. Surf. Sci. Catal.* **1994**, *83*, 49.
(16) Schoeman, B. J.; Sterte, J.; Otterstedt, J.-E. *Zeolites* **1994**, *14*, 110.
(17) Otterstedt, J.-E.; Sterte, J.; Schoeman, B. J. Swedish Patent Application 92 02 518-8, 1992.
(18) Schoeman, B. J.; Sterte, J.; Otterstedt, J.-E. *J. Colloid Interface Sci.* **1995**, *170*, 449.
(19) Schoeman, B. J.; Sterte, J.; Otterstedt, J.-E. *Zeolites* **1994**, *14*, 557.
(20) Fang, M.; Du, H.; Xu, W.; Meng, X.; Pang, W. *Microporous Mater.* **1997**, *9*, 59.
(21) Flanigen, E. M.; Bennet, J. M.; Grose, R. W.; Cohen, J. P.; Patton, R. L.; Kirchner, R. M.; Smith, J. V. *Nature* **1978**, *271*, 512.
(22) Twomey, T. A. M.; Mackay, M.; Kuipers, H. P. C. E.; Thompson, R. W. *Zeolites* **1994**, *14*, 162.
(23) Cundy, C. S.; Lowe, B. M.; Sinclair, D. M. *J. Cryst. Growth* **1990**, *100*, 189.
(24) Dokter, W. H.; van Garderen, H. F.; Beelen, T. P. M.; van Santen, R. A.; Bras, W. *Angew. Chem., Int. Ed. Engl.* **1995**, *34*, 73.
(25) Bodart, P.; Nagy, J. B.; Gabelica, Z.; Derouane, E. G. *J. Chim. Phys.* **1986**, *83*, 777.
(26) Ciric, J. *J. Colloid Interface Sci.* **1968**, *28*, 315.

(27) Freund, E. F. *J. Cryst. Growth* **1976**, *34*, 11.
(28) Scott, G.; Thompson, R. W.; Dixon, A. G.; Sacco, A. *Zeolites* **1990**, *10*, 44.
(29) Larson, A. C.; von Dreele, R. B. *GSAS, General Structure Analysis System*; LANSCE, MS-H805; Los Alamos National Laboratory: Los Alamos, NM.
(30) van Koningsveld, H.; van Bekkum, H.; Jansen, J. C. *Acta Crystallogr*. **1987**, *B43*, 127.
(31) Brunauer, S.; Emmett, P. H.; Teller, E. J. *J. Am. Chem. Soc.* **1938**, *60*, 309.
(32) Lewellyn, P. L.; Grillet, Y.; Patarin, J.; Faust, A. C. *Microporous Mater*. **1993**, *1*, 247.
(33) Lipens, B. C.; de Boer, J. H. *J. Catal.* **1965**, *4*, 319.
(34) Corkery, R. W.; Ninham, B. W. *Zeolites* **1997**, *18*, 379.
(35) Detailed results of the Rietveld refinements are available in Supporting Information.
(36) van Konningsveld, H.; Jansen, J. C.; van Bekkum, H. *Zeolites* **1990**, *10*, 235.
(37) Boxhoorn, G.; van Santen, R. A.; van Erp, W. A.; Hays, G. R.; Huis, R.; Clague, D. *J. Chem. Soc., Chem. Commun.* **1982**, 264.
(38) Nagy, J. B.; Gabelica, Z.; Derouane, E. G. *Chem. Lett.* **1982**, 1105.
(39) Nagy, J. B.; Gabelica, Z.; Debras, G.; Bodart, P.; Derouane, E. G.; Jacobs, P. A. *J. Mol. Catal.* **1983**, *20*, 327.
(40) Boxhoorn, G.; Kortbeek, A. G. T. G.; Hays, G. R.; Alma, N. C. M. *Zeolites* **1984**, *4*, 15.
(41) Fyfe, C. A.; Gobbi, G. C.; Klinowski, J.; Thomas, J. M.; Ramdas, S. *Nature* **1982**, *296*, 530. Fyfe, C. A.; Grondey, H.; Feng, Y.; Kokotailo, G. T. *J. Am. Chem. Soc.* **1990**, *112*, 8812.
(42) Parker, L. M.; Bibby, D. M.; Patterson, J. E. *Zeolites* **1984**, *4*, 168.
(43) Gilson, J. P.; Derouane, E. G. *J. Catal*. **1984**, *88*, 538.
(44) Woolery, G. L.; Alemany, L. B.; Dessau, R. M.; Chester, A. W. *Zeolites* **1984**, *6*, 14.
(45) Scarano, D.; Zecchina, A.; Bordiga, S.; Geobaldo, F.; Spoto, G.; Petrini, G.; Leofanti, G.; Padovan, M.; Tozzola, G. *J. Chem. Soc., Faraday Trans.* **1993**, *89* (22), 4123.
(46) Zecchina, A.; Bordiga, S.; Spoto, G.; Marchese, G.; Petrini, G.; Leofanti, G.; Padovan, M. *J. Phys. Chem.* **1992**, *96*, 4985.
(47) Jacobs, P. A.; Beyer, H. K.; Valyon, J. *Zeolites* **1981**, *1*, 161.
(48) Coudrier, G.; Naccache, C.; Vedrine, J. C. *J. Chem. Soc., Chem. Commun*. **1982**, 1413.
(49) Testa, F.; Szostak, R.; Chiappetta, R.; Aiello, R.; Fonseca, A.; Nagy, J. B. *Zeolites* **1997**, *18*, 106.
(50) Nagy, J. B.; Gabelica, Z.; Derouane, E. G. *Zeolites* **1983**, *3*, 43.